WAFER-LEVEL INTEGRATED ELECTROSPRAY EMITTERS FOR A PUMPLESS MICROTHRUSTER SYSTEM OPERATING IN HIGH EFFICIENCY ION-MODE

Caglar Ataman, Simon Dandavino and Herbert Shea
LMTS, Ecole Polytechnique Fédérale de Lausanne (EPFL), SWITZERLAND

ABSTRACT

Microfabrication, wafer-level integration, and characterization of internally fed arrays of electrospray thrusters for spacecraft propulsion are discussed. 5 µm inner diameter, 100 µm long capillaries and 150-to-300 µm diameter annular extractor electrodes are integrated vertically via a polymer based wafer bonding process, allowing high yield and post testing disassembly of the bonded stack. The small inner diameter of the capillaries allows passive, capillary force driven delivery of the propellant to the emission site, and therefore potentially eliminating the need for an active pump system. The fabricated thruster chips were successfully tested in pumpless liquid delivery configuration under unipolar and bipolar excitation.

INTRODUCTION

Maneuverable Pico (1-10 kg mass) and Nano (10-100 kg mass) satellites employing microthrusters have the potential to revolutionize space exploration missions by allowing cost and time effective access to space. The critical performance criteria for a microthruster targeting pico/nano satellites is the specific impulse (I_{sp}), which is a measure of increase in satellite momentum per unit propellant consumption. Electrospray thrusters operating in purely ionic mode outperform any other rivaling thruster technology in this regard, but they suffer from a fundamental trade-off between the I_{sp} and the thrust. Our group has previously developed an array of electrospray emitters using microfabrication that has the potential to combine the very high I_{sp} of this method with sizable thrust [1, 2]. Moreover, ion mode operation from an internally wetted capillary type electrospray system was proven for the first time to our knowledge by tailoring the capillary hydraulic impedance by silica bead filling [2]. However, this was a tedious process that resulted in unrepeatable capillary tip profiles, therefore limited the flexibility in array sizes. Furthermore, the manual assembly of the thrusters was sensitive to contamination and had low yield. In this paper, we present a new generation of thrusters with much smaller capillary diameters and a higher level of integration, and demonstrate bipolar ion-mode operation with liquid delivery via capillary forces only. This is a major step towards a pumpless system, which could significantly simplify thruster design and flight procedures.

DESIGN AND OPERATION

The operation principle of an electrospray thruster and the microfabricated thruster structure are depicted in Figure 1. In the most basic configuration, an electrospray thruster consists of a capillary filled with a conductive ionic liquid (EMI-BF4 in this case) and a hollow extractor electrode placed at close proximity of the capillary tip. With high potential difference in the order of a kV applied between the liquid and the extractor, the tip meniscus collapses into a Taylor cone, leading to the emission of high energy droplets and/or ions from the cone apex. The acceleration of these massive particles exerts a reaction force on the spacecraft that thrusts it in the opposite direction.

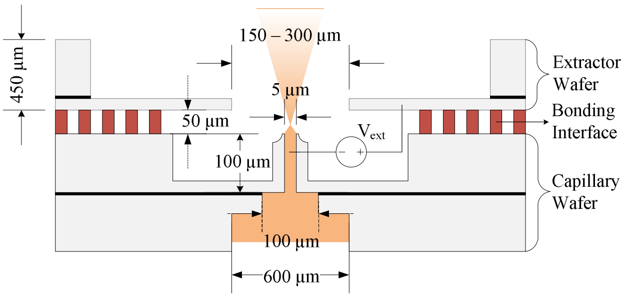

Figure 1: Cross-section view of the integrated thruster module depicting the thruster operation principle. The beam emission is induced by the large potential difference applied between the liquid and the extractor.

The thruster chips developed in this work consist of an emitter and an extractor integrated with a 50 µm thick polymer layer in between. The capillaries stand off the silicon surface and each face an individual annular extractor electrode. The intention of this layout is to guarantee homogeneous spray characteristics across the array. The extractor electrode chip is electrically isolated from the capillary one by the said polymer layer.

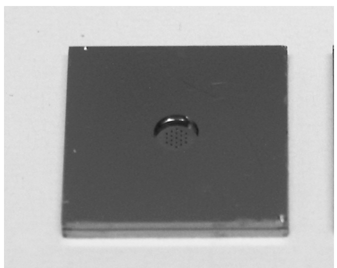

Figure 2: Photo of a thruster chip with 19 emitters, seen from the extractor side. The chip is 10 x 10 mm in size.

FABRICATION PROCESS

The fabrication of the emitters and the extractors are based on silicon-on-insulator (SOI) wafers from a commercial supplier. For both the capillaries and the emitters, the process begins with thermal oxidation (2.2 µm). The first lithography, wet oxide etch and the consecutive Deep Reactive Ion Etch (DRIE) defines the extractors on the device layer of the extractor wafer, which has 50/2/400 µm thick device/oxide/handle layers (Figure 3b). The extractor dimensions vary from 75 µm to 200 µm. A similar set of steps follow for the opening of the extractors from the backside. The thick handle layer acts both as a support layer for the relatively thin extractors and also as a spacer with well-defined thickness between the extractors and a possible integrated accelerator electrode. Finally, the buried oxide and the remaining oxide layers on both faces are removed and the wafers are coated with 200 nm of aluminum on both sides to maintain uniform potential distribution on the extractor chip (Figure 3c).

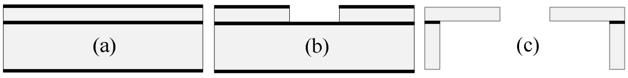

Figure 3: Fabrication steps for the extractor wafers. The SOI wafers have 50 µm thick device layer, 2 µm thick buried oxide layer and 400 µm thick handle layer.

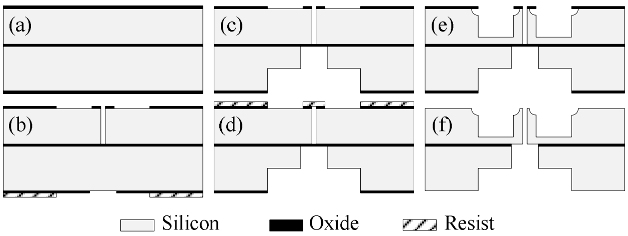

Figure 4: Fabrication steps for the extractor wafers. The SOI wafers have 100 µm thick device layer, 2 µm thick buried oxide layer, and 500 µm thick handle layer. The thermal oxide on both faces is 2.2 µm thick.

Capillary Fabrication

The process for the capillaries involves four lithography and etching steps, and is summarized in Figure 4. A silicon-on-insulator (SOI) wafer with 100/2/500 µm top silicon/isolating oxide/bottom silicon layers is used as the substrate. Via the first lithography/wet oxide etch/DRIE sequence the 100 µm deep capillaries are defined on the device layer. This etch constitutes the most critical step within the process flow due to the high aspect ratio required (Figure 4b). The optimization of the etch parameters is of utmost importance to ensure small capillaries with high hydraulic impedance. Following the capillary etch, the two-level liquid reservoir is formed on the handle layer using DRIE with stacked photoresist and oxide mask (Figure 4c). For the lithography defining the outer capillary walls, a 6.9 µm thick AZ9260 photoresist layer is used, since it provides good coverage over the structured surface (Figure 4d). The emitters are then shaped by an isotropic silicon etch (to increase tip sharpness) and a consecutive DRIE step (Figure 4e). The capillary fabrication is completed by the release of the chips in a wet oxide etching bath (Figure 4f). An SEM image of a single emitter is given in Figure 5.

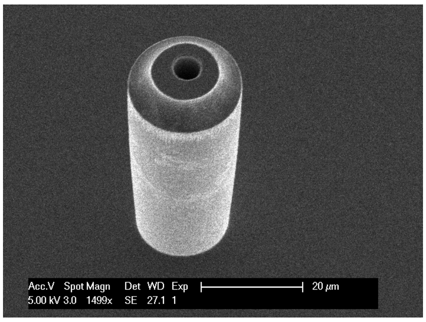

Figure 5: SEM Image of a single emitter with an inner diameter of 5µm and outer height of 70 µm.

Wafer-Level Integration

For wafer level integration, a new bonding process was developed using DuPont MX5000 series laminated dry photoresist (Figure 6b). Using this resist as the bonding agent yields an isolating and high dielectric strength (>3 kV experimental) bonding interface with thicknesses well-suited for the desired thruster configuration (15 to 50 µm). The bonding is reversible, allowing the detailed inspection of the thruster constituents after testing. The quality of the bonding was qualitatively assessed by the percentage of the chips that remain bonded after dicing. By optimizing the bonding parameters (such as surface treatment, bonding temperature and pressure) 100% post-dicing yield can be achieved.

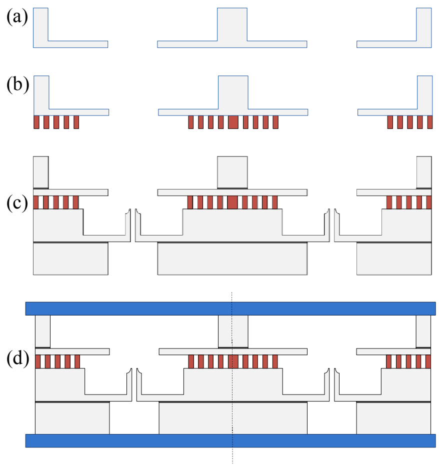

Figure 6: The 50 µm thick dry resist enables post-fabrication bonding of the fully processed capillary and extractor wafers, since it can be laminated and patterned on structured surfaces.

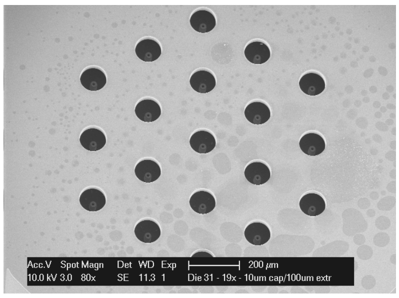

Figure 7: SEM Image of an integrated thruster array with 19 emitters.

EXPERIMENTAL RESULTS

Test Setup

The test bench consists of a vacuum chamber for thrust performance characterization and a second chamber for test liquid storage (Figure 8). The storage of ionic liquid in vacuum avoids bubble formation during thruster filling. Both chambers are connected through a silica capillary tube to transfer the liquid from the reservoir to the thruster. For spray testing, the emitter capillaries are connected to a high voltage source. During all tests the extractor electrodes are grounded and the emitter capillaries biased to high voltage. The electrospray current is measured by means of a Faraday cup, which is monitored using a Keithley 6487 pico-ammeter. For rapid and accurate measurements, the test setup is fully computer-controlled.

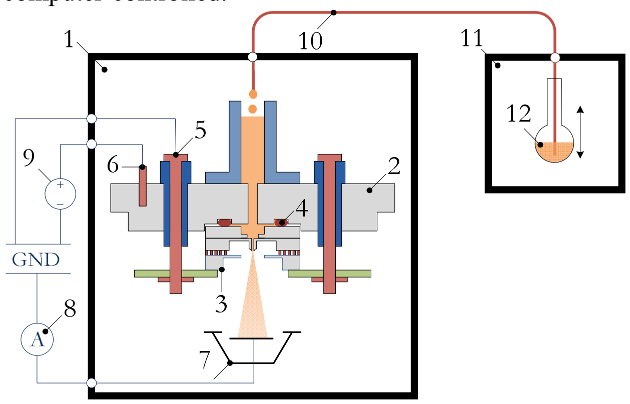

Figure 8: Schematic of the test rig for thruster characterization. 1) Main chamber 2) Chip Holder 3) Thruster chip 4) O-Ring 5)Extractor addressing 6) Liquid addressing 7) Faraday cup 8) Pico-ammeter 9) High voltage source 10) Glass capillary 11) Liquid chamber 12) Liquid reservoir

The thruster chips are placed into the test chamber with a simple assembly that provides the electrical and fluidic interfaces. For the containment of the liquid, a simple EPDM rubber O-ring is used between the thruster module and the aluminum chip holder providing a tight seal when the thruster module is fastened in place by a laser machined steel plate. This steel plate is in contact with the extractor electrode, providing the first electrical lead. The liquid is addressed through the aluminum chip holder.

Unipolar Operation

In Figure 9, the average current as a function of liquid voltage is plotted for a 5/150 µm capillary/extractor diameter thruster using EMI-BF_4 ionic liquid at room temperature and under negative unipolar excitation. The voltage was swept with 1 V steps to minimize transients and ensure quasi-static operation. The hysteresis in the I-V curve is attributed to the initial concave shape of the liquid meniscus. Due to this shape, the formation of the Taylor cone is delayed. However, once the Taylor cone is formed, which is the case for the downsweep, it can be maintained with a lower electrostatic filed.

The evolution of the spray behavior as a function of increasing liquid voltage is depicted in Figure 10. The spray is initiated in the pulsation mode at 560 V with the pulse frequency, strength and width increasing with increasing voltage. In the transition region between the pulsation and stable modes, the repeatability of the pulses disappears and the behavior is non-predictable. At Around 740, the spray is completely stable with high ion-composition, making this range the preferable operation regime for a high-efficiency thruster system.

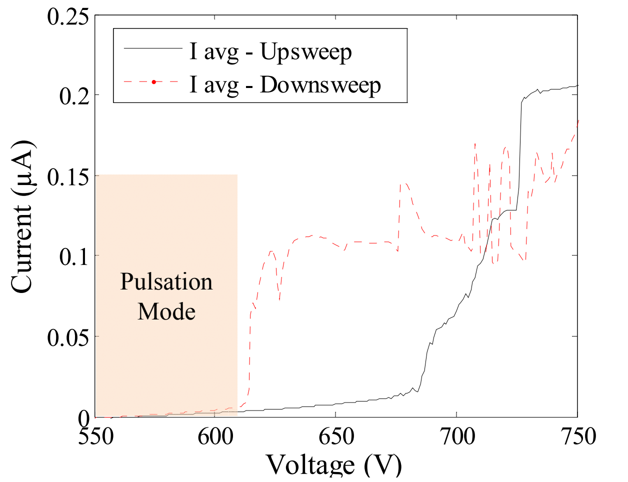

Figure 9: Unipolar I-V curve with negative liquid voltage (negative ion emission) and a possible operation window with stable emission current. The hysteresis in the I-V curve is clearly observable.

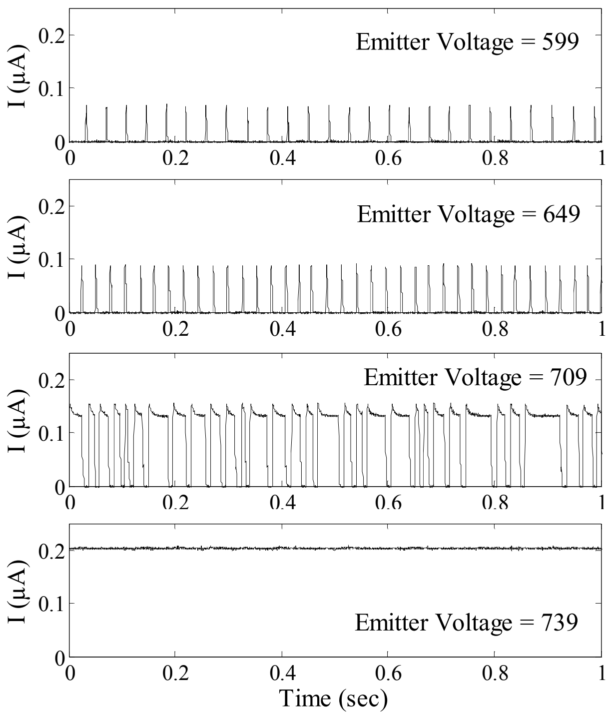

Figure 10: Evolution of the spray behavior with the liquid voltage increased quasi-statically.

Bipolar Operation

In Figure 11, the I-V curve for a 5/150 µm capillary/extractor diameter thruster using EMI-BF4 ionic liquid at room temperature and bipolar excitation. The extractor voltage was a bipolar square signal with 0.5 Hz frequency and varied amplitude. Every data point on Figure 11a represents the average spray current at the positive or negative potential region of a single period. The current levels are significantly lower, when compared to Figure 10, due to some additional grids placed in front of the Faraday cup, reducing the collected current by a factor of four to five. The slight asymmetry of the spray current for the positive and negative cycles is attributed to the different atomic mass of the extractor ions. As in the unipolar mode, the spray initiates in the pulsed mode and gradually transforms into stable operation with increasing amplitude. In Figure 11b, the transient behavior of the spray current can be observed. At 575V, the electrospray is in pulsed mode producing current pulses with a repeatable amplitude and period. With increasing extractor voltage, the spray gradually evolves into a more stable form.

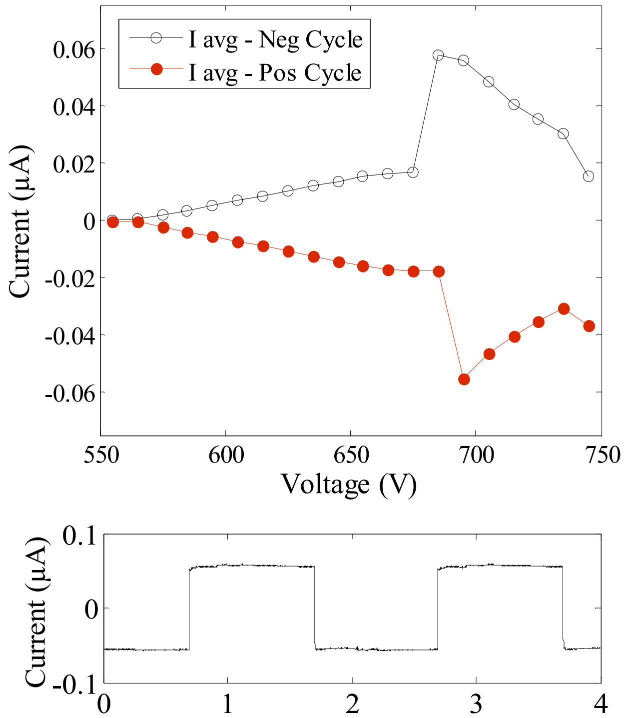

Figure 11: (a) I-V curve for a single 5 µm inner diameter emitter with passive liquid delivery and power supply polarity alternating at 0.5 Hz. The stable bipolar emission is observed starting from 695V. The current trace at this voltage is depicted in (b).

CONCLUSIONS

Microfabrication, assembly, and characterization details for the first iteration MEMS thruster chips are presented in this deliverable report. The fundamental enabling features of these chips are the small (5µm) inner diameter of the capillaries, and the wafer-level integration of the chips components. By reducing the capillary diameter, it was aimed to obtain high hydraulic impedance, which is necessary to reach ionic-mode operation. Integrated fabrication of the chips with the extractor and the capillary layers significantly facilitates the post-processing and testing of the chips, since it eliminates the need of manual alignment and assembly. The bonding is reversible, allowing the detailed inspection of the thruster constituents after testing. The quality of the bonding was qualitatively assessed by the percentage of the chips that remain bonded after dicing. By optimizing the bonding parameters (such as surface treatment, bonding temperature and pressure) 100% post-dicing yield is demonstrated. The fabricated thruster chips were successfully tested in pumpless liquid delivery configuration. Stable bipolar operation with passive liquid delivery and ionic-mode operation with passive liquid delivery have been successfully demonstrated.

ACKNOWLEDGEMENTS

This work has been supported by the MicroThrust project, grant agreement number 263035, funded by the EC Seventh Framework Programme theme FP7-SPACE-2010 (www.microthrust.net).

REFERENCES

[1] Krpoun, Renato, H. R. Shea. “Integrated out-of-plane nanoelectrospray thruster arrays for spacecraft propulsion.” Journal of Micromechanics and Microengineering 19, no. 4 (April 2009): 045019.

[2] Krpoun, Renato, Katharine Lucy Smith, John P. W. Stark, and H. R. Shea. “Tailoring the hydraulic impedance of out-of-plane micromachined electrospray sources with integrated electrodes.” Applied Physics Letters 94, no. 16 (2009): 163502.

CONTACT

*C. Ataman, tel: +41-32-7205357;
caglar.ataman@epfl.ch